Research Report

Direct Observation of Adsorption Reactions of Ti on Si(001)-2 × 1 by Scanning Tunneling Microscopy

Kengo Ishiyama, Yasunori Taga, Ayahiko Ichimiya

Abstract

We have used a scanning tunneling microscope (STM) to determine a site conversion path of a Ti atom on the Si(001)-2 × 1 surface and the activation energies. We have found that adsorption of Ti between 442 K and 488 K is described by two precursor states and a final state. A Ti adatom is converted reversibly between the two precursor states, i.e., the pedestal site adsorption and a highly mobile state between the dimer rows. In contrast, the final state, i.e., the vacancy site adsorption is created only from the pedestal site adsorption. By counting individual events of two types of the site conversions, i.e., one from the pedestal site adsorption to the vacancy site (type-A) and another to the highly mobile state (type-B), we have obtained activation energies of E_A = 1.6 ± 0.1 eV and E_B = 1.6 ± 0.2 eV for type-A and type-B, respectively. The conversion paths and the deduced activation energies are consistently interpreted in terms of the local bonding nature of a Ti adatom on the Si dimer reconstruction.

Keywords: Scanning tunneling microscopy, Silicon, Titanium, Surface chemical reaction, Surface diffusion, Adatom, Metal semiconductor interfaces

1. Introduction

For both fundamental and technological reasons, transition metal (TM) silicides have been studied extensively. Especially Ni/Si(111) and Co/Si(111) systems have been major subjects for both experimental and theoretical investigations[1-6]. This is because Ni- and Co-silicides grow epitaxially as single-crystal overlayers, hence, they have been prototypes for characterizing their interfacial structures and the correlation between the structures and the electronic properties represented by Schottky-barrier heights. Contrasting to the above near-noble metals, strong bonding between Ti and Si has been shown as a spontaneous Ti-Si mixing upon deposition of Ti on a Si substrate at room temperature [7-10]. The variation of reactivity between TM's and Si is often explained in terms of the interactions between the *d* orbital of TM's and the 3*p* orbital of Si[11]. Based on this concept, Ti 3*d* orbital and Si 3*p* orbital hybridize to form a partially filled bonding state and an unfilled non-bonding state and an anti-bonding states, which lowers the total energy. On the contrary, extra Ni 3*d* electrons would go into a non-bonding state, which raises the total energy. This means that there is a trend that Ti forms strong bonds with Si compared to Ni does. The Ti-Si bonding interaction would induce significant changes of bonding configurations at the Ti/Si interface and likely causes the breakage of Si-Si bonds. It is also likely that the weak bonding of Ni and Si causes the higher diffusivity in Si compared to that of Ti[12]. Nevertheless, the past experimental studies could not provide direct evidences of such TM-Si interactions at the atomic scale because of the limited space resolution.

To reveal the Ti-Si reaction mechanisms at the atomic scale, we employed scanning tunneling microscopy (STM)[13]. We found two distinct adsorption sites of Ti adatoms dependent on temperature. Below 440 K, a Ti atom adsorbs at the pedestal site highly preferentially. Above 440 K, a Ti adatom adsorbs at the second layer of Si. By observing site conversion and the simultaneous growth of Si dimer islands *in situ*, we modeled that a site conversion of a Ti adatom from the top surface to the second layer of Si induces ejection of Si dimer atoms. It is considered that these observations are direct evidences of the above inferred mechanism for substrate disruption, and a precursor to a silicidation reaction.

In the present study, we focus our attention particularly on giving an overall description of adsorption behavior of Ti on the Si(001)-2 × 1 surface. First, we show STM observations of site conversions including newly reported ones. Second, we describe measurements of the site conversion rates and determination of the activation energies. With the results, we discuss the conversion mechanisms in terms of the bonding nature of a Ti adatom with the Si surface and attempt to give an integrated view of the reaction path. To our knowledge, this work is the first example which provides a description of a reacting TM/Si interface based on the direct imaging in the atomic resolution and a quantitative evaluation of the reactions.

2. Experiment

STM measurements were carried out in an ultra-high-vacuum (UHV) chamber equipped with a commercial scanning tunneling microscope (JEOL JSTM-4500VT) and a micro-beam Ti evaporation source. A Si(001) substrate (Sb doped, 0.01 Ωcm, 22 × 3 × 0.3 mm^3) was cleaned by a wet chemical process and was introduced to the UHV chamber. The sample was resistively heated to 920 K for 10 h to degas the sample and the holder before quick flash at 1500 K. The temperature was monitored through a CaF_2 window with an infrared thermoviewer, which was previously calibrated with a WRe thermocouple with an accuracy of about ±5K. The STM measurement was carried out in a temperature range of 442 - 488 K. The glancing angle of incident Ti flux was set at 5° so that Ti flux could reach the scanning area only by retracting the W probe tip ~1000 Å away from the surface. When the drift rate of the image decreased down to < 0.1 Å s^{-1} in 1 - 2 h after providing the heating current, the probe tip was retracted away and Ti was evaporated. Relatively low Ti coverages of 0.01 - 0.02 ML were used to avoid possible interactions of Ti adatoms. Immediately after the deposition, a sample area of 500 × 500 $Å^2$ was scanned successively at 18 s intervals in a “successive-scan method”, and 240 - 360 s intervals during which the probe tip was retracted ~ 1000 Å away in an “interval-scan method.” The sample bias of ~+1 V and the tunneling current of 0.1 nA were used. The system pressure was maintained at about 1 - 2 × 10^{-10} Torr during the Ti evaporation and high temperature observations.

3. Result

3. 1 Observations of site conversions

We have found three distinct types-A, -B, and -C of site conversions by direct imaging as follows.

Fig. 1 shows a series of STM images taken successively at 18 s intervals immediately after the Ti evaporation at 466 K. In Fig. 1(a), four bright protrusions labeled P on dimer rows are Ti adatoms at the pedestal sites. In the following scans, the bright spots change into distinctive dark spots labeled V. The displacement between the sites before and after the conversion is a half of the dimer-dimer spacing of 3.8 Å. The dark spot is Ti adsorption at a dimer vacancy which is created

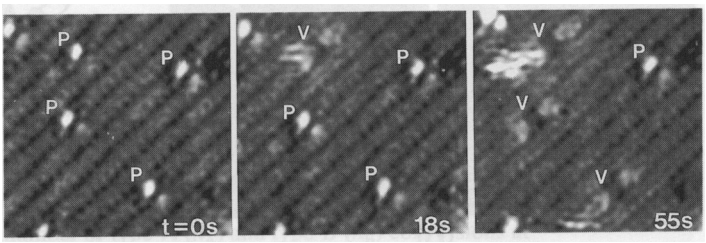

Fig. 1 Type-A conversion ; conversions from the pedestal site adsorption (P) to the vacancy site adsorption (V) of Ti adatoms on the Si(001)-2 × 1 dimer rows. Images are taken immediately after Ti deposition at 466 K of about 0.01 ML at intervals of 18 s. The sample bias is +0.8 V. Image size is 80 × 80 $Å^2$.

simultaneously with the site conversion[13]. This adsorption structure survives up to 630 K without significant structural changes except for its diffusion motion[13]. This site conversion is hereafter called a type-A.

In **Fig. 2**(a), a Ti adatom arrowed at t = 0 disappears in the next scan after 18 s. At the same time, a Ti adatom appears ~70 Å away on the dimer row on which the disappearance occurs. In Fig. 2(b), disappearance and appearance of Ti adatoms take place ~90 Å apart from each other on the neighboring dimer rows. We observed about 200 disappearance events in the conversion rate measurement described below, and we observed only several cases in which the disappearance and appearance took place within two successive scans. In most cases, only disappearance or appearance of a Ti adatom was seen in a single scan. Hereafter, the disappearance of a Ti adatom is called a type-B conversion, and the appearance of a Ti adatom a type-C conversion. Different types of site conversions of monatomic adsorption other than the above three types have not been observed. Therefore, we conclude that the above three types are the major site conversions of a Ti adatom on the Si(001)-2 × 1 in the experimental temperature range.

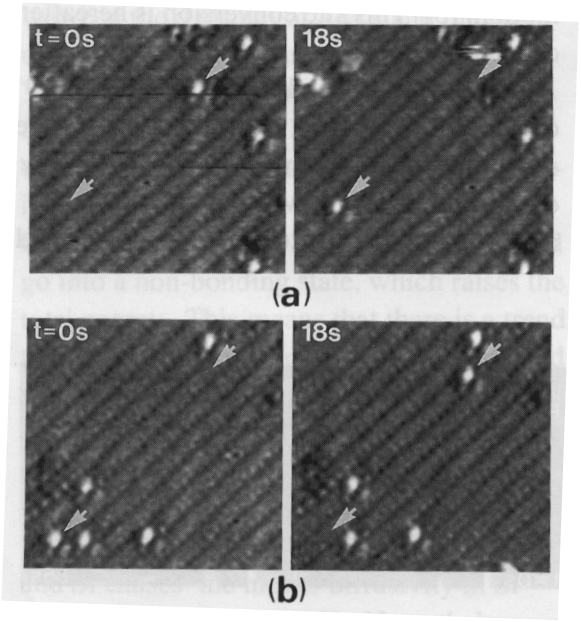

Fig. 2 Two sets of disappearance (type-B conversion) and appearance (type-C conversion) of Ti adatoms which take place within a scan interval of 18 s at 466 K. Image size is 100 × 100 Å^2.

3. 2 Measurement and analysis of site conversion rates

For estimating rates of the site conversions including the type-C conversion, an unobservable state before the type-C conversion is necessarily taken into consideration. However, as discussed below in detail, it is thought that the "invisible" state would contribute to the growth of clusters shown in our previous paper. A model involving such a nucleation process would be too confusing to be analyzed. Therefore, we restrict ourselves to evaluate the conversion rates of the type-A and the type-B, thus only values observable with a minimum uncertainties are required.

At a certain temperature T (K), we chose N_P (= 50 - 100) adatoms at the pedestal sites at t = 0. We measured the number of the site conversions $n_A(t,T)$ and $n_B(t,T)$ which occurred among N_P adatoms from t = 0 to t, by counting individual conversion events in many successive images. Denoting conversion rates for type-A by $\nu_A(T)$ and type-B by $\nu_B(T)$, rate equations for the site conversions are simply written as

$$\begin{cases} \dfrac{\partial n_A}{\partial t} = (N_P - n_A(t,T) - n_B(t,T))\nu_A(T) \\ \dfrac{\partial n_B}{\partial t} = (N_P - n_A(t,T) - n_B(t,T))\nu_B(T) \end{cases} \cdots (1)$$

The simultaneous equations yield two relationships, such as,

$$n_A(t,T) + n_B(t,T) = N_P(1 - \exp(-(\nu_A(T) + \nu_B(T)))) \cdots\cdots\cdots (2)$$

and

$$\frac{\nu_i(T)}{\nu_A(T) + \nu_B(T)} = \frac{n_i(t,T)}{n_A(t,T) + n_B(t,T)} \cdots (3)$$

Here, i = A or B. As shown in **Fig. 3**(a) and (b), the measured time evolution of $n_A(t,T)$ and $n_B(t,T)$ at each temperature are well fitted by exponential decay curves as modeled above. From the measurements of $n_A(t,T)$ and $n_B(t,T)$ at various temperatures between T = 442 K and 488 K, we estimated conversion rates $\nu_A(T)$ and $\nu_B(T)$. We show an Arrhenius plot of the result in Fig. 3(c). The measured values

of $\nu_A(T)$ and $\nu_B(T)$ are well fitted by almost parallel straight lines. By the least square fit, we obtain activation energies and prefactors, E_A = 1.6 ± 0.1 eV and $\nu_{A0} = 10^{14\pm1}s^{-1}$ for the type-A, and E_B = 1.6 ± 0.2 eV and $\nu_{B0} = 10^{14\pm2}s^{-1}$ for the type-B. Due to the error range, we cannot discriminate which, the activation energy or the prefactor, causes the difference in the rates of the two types of site conversions in the experimental temperature range.

4. Discussion

4. 1 Estimation of a tip-effect

Here we discuss a possible tip-surface interaction which might influence the measured rate of the site conversion. Because the temperature dependence of a possible tip-surface interaction is not known, we restrict ourselves to estimate the tip effect only in terms of tip-surface interaction time. As has been presented by many experimental and theoretical studies, a tip-surface interaction is induced in the vicinity of the small tunneling gap[14]. Hence, we define tip-surface interaction time to be a period during which the tip is within the tunneling region from the surface per unit measurement time. For the successive-scan method, an interaction time t_s =1, while that in the interval-scan method t_i = 18/240 - 18/360. Therefore, by using the interval-scan method, a possible tip-effect on the site conversions is reduced by a ratio t_s / t_i =13 - 20.

As shown in Fig. 3, the discrepancy between the conversion rates obtained by the two scan methods does not exceed the measurement error range. This indicates a negligible tip effect in the experimental temperature range, as long as the tip effect does not have a temperature dependence larger than that given as a constant change of the activation energy or the prefactor. In addition, the obtained prefactors agree with many reported experimental values and the popularly perceived effective prefactor of the order of 10^{12} - 10^{13} s^{-1} (Refs.15-17). Therefore, we judge that a possible tip-surface interaction does not give an influence larger than the experimental error range of measurements.

4. 2 Site conversion paths and activation energies

Below, we estimate a site conversion path of a Ti adatom on the surface, and show the result in **Fig. 4**.

First, the vacancy site adsorption formed by the type-A conversion does not show structural change in the present experimental temperature range. Therefore, the vacancy site adsorption is regarded to be the final state of the whole site conversion path. An “invisible” state after detachment from and before attachment to the pedestal site is estimated as follows. A Ti adatom does not show any mobility along the pedestal sites in a row before a type-A or a type-B conversions. This indicates that a potential barrier for the displacement path without inducing a type-A conversion (E_P), for example, a path above the level of dimer atoms, is higher than that for the

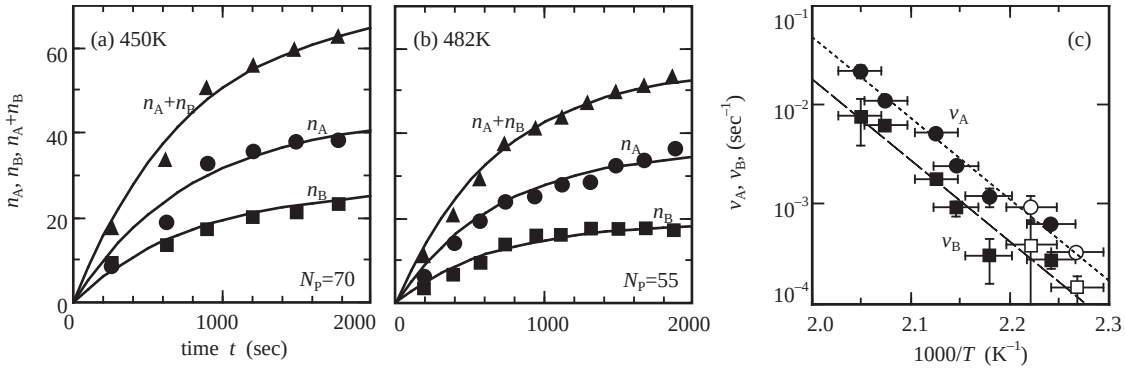

Fig. 3 Time evolution of the number of type-A (n_A) and type-B (n_B) conversions at (a) 450 K and (b) 482 K. Curves for each temperature are written by $n_i(t) = n_i(\infty)$ (1-exp(–νt)), i = A or B, with a common ν. (c) An Arrhenius plot of the conversion rates for type-A (ν_A) and type-B conversions (ν_B). Open symbols are data points obtained by an interval-scan method. The obtained activation energies and prefactors are E_A = 1.6 ± 0.1 eV and $\nu_{A0} = 10^{14\pm1}s^{-1}$ for type-A, and E_B = 1.6 ± 0.2 eV and $\nu_{B0} = 10^{14\pm2}s^{-1}$ for type-B.

type-A and the -B conversions. In other words, the dimer row is described as a row of potential wells deeper than 1.6 eV. Consequently, it is highly likely that the "invisible" state of Ti is one-dimensional fast migration along the sites located between the dimer rows which is labeled D. Therefore, the type-B and the type-C conversions are attributed to be displacement of a Ti adatom between the pedestal site and a site between the dimer rows. Thus type-B and type-C are regarded to be reverse processes of each other, and the pedestal site adsorption and the highly mobile state between the dimer rows are to be precursor states to the final vacancy site adsorption. Based on this interpretation, it is likely that the observations shown in Fig. 2 are snapshots before and after a sequence of a type-B, D, and -C conversions of a single Ti adatom. In addition, the rare occurrence of pairs of the type-B and type-C conversions suggests that the most probable migration range is considerably larger than the scan size of 500 Å. It is considered that Si adatoms created by the type-A conversion also have high mobility[15]. Therefore, the fast migrating Ti and Si adatoms probably meet with the other adatoms to form clusters and/or are captured by existing clusters.

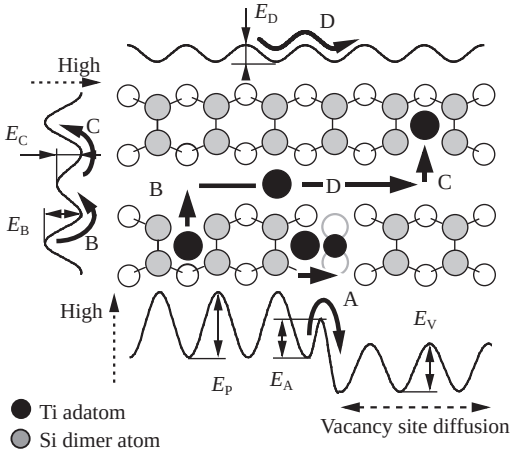

Fig. 4 Models for site conversion paths and corresponding potential curves. The curves shown indicate relative height of the potential along conversion paths and a migration path between the dimer rows (labeled E). For E_P, E_C and E_E, only relative height to the measured values are estimated. The activation energy for the diffusion of vacancy site adsorption structure (E_V =1.8eV) is also shown.

We are able to estimate relative heights of the potential barriers along the site conversion path of a Ti adatom as shown in Fig. 4. First, the potential barrier for type-A (E_A) and type-B (E_B) conversions are measured to be ~1.6eV, as shown above. The highly preferred adsorption of Ti at the pedestal site at room temperature[13] suggests that a conversion rate of type-C is higher than that of type-B at room temperature. Assuming that the Arrhenius law is valid from room temperature to the present experimental temperature range, this corresponds to that the potential barrier for type-C (E_C) is lower than that for type-B (E_B). The high mobility of a Ti adatom along the sites between the dimer rows indicates that the potential barrier for migrating between the dimer rows (E_D) is smaller than those for the other conversion paths. Then, the above estimation is summarized as

$$E_P > E_A \approx E_B > E_C > E_D. \quad \cdots\cdots\cdots\cdots (4)$$

We cannot judge so far which is larger E_P or E_V; the diffusion activation energy of the vacancy site adsorption[13].

Finally, we attempt to give a qualitative interpretation for the measured activation energies based on models for bonding sequences during the site conversions in **Fig. 5**. At the initial pedestal site of the type-A conversion, a Ti adatom forms bonds with four dimer atoms (1, 1', 2, 2'). At the next stage II, the Ti adatom moves to the right, and finally sinks to the second layer at stage III. On the displacement path of a Ti adatom, the forward dimer bond opens and/or the dimer backbonds stretch to allow the Ti atom to move down. It is likely that at this stage the dimer backbonds at the dimer atoms (2, 2') are thermally broken, and Si dimer atoms are ejected as derived from the observations[13]. The type-B conversion is modeled as shown in Fig. 5(b). When the Ti adatom moves off the center of the dimer row at stage II, bonds between the Ti adatom and the backward dimer atoms (1, 2) are broken. At stage III, the two backbonds of the Ti adatom are broken and the Ti adatom falls between the dimer rows.

As seen clearly, both models involve breakage of

bonds between the Ti adatom and Si dimer atoms backward of the displacement direction. At such a transient bonding configuration, a large lattice strain and a decrease of the number of bonds should be induced and cause an increase of potential energy. Therefore, it is highly likely that the bond-breakage processes determines the similar potential barriers for the two site conversions. In contrast, the estimated low potential barrier for a migration along the sites between the dimer rows is interpreted to be due to the weak bonding between a Ti adatom and Si atoms with fully saturated bonds. Also, this probably causes the higher potential energy at the sites between the dimer rows, which should lead the potential barrier for type-C lower than that for type-B, as schematically shown in Fig. 4.

5. Conclusion

Direct imaging of site conversions of Ti adatoms on the Si(001)-2 × 1 surface and direct rate measurements have enabled us to provide an integrated view of a site conversion path and the kinetics. It is revealed that the behavior of adsorption reactions and diffusion is determined by the local bonding nature associated with the dimer reconstruction. In addition, it is suggested that the fast migrating Ti adatoms should play an important role in the nucleation growth of silicides by evaporation. Thus, the present observations and interpretation of the atomic processes of Ti adsorption on the Si(001) surface provide an important insight into the growth process of the titanium silicide under complex contributions of the adsorption reactions and diffusion of adatoms.

Acknowledgments

We acknowledge our colleague K. Miwa at Toyota Central Res. and Develop. Labs., Inc., for valuable discussions with insightful suggestions from a theoretical point of view.

References

1) Rangelov, G., Augustin, P., Stober, J. and Fauster, Th. : Phys. Rev. B, **49**(1994), 7535
2) Vrijmoeth, J., van der Veen, J. F., Heslinga, D. R. and Klapwijk, T. M. : Phys. Rev. B, **42**(1990), 9598
3) Bennett, P. A., Copel, M., Cahill, D., Falta, J. and Tromp, R. M. : Phys. Rev. Lett., **69**(1992), 1224
4) Lee, E. Y., Sirringhaus, H. and von K¨ånel, H. : Surf. Sci., **314**(1994), L823
5) Tsai, M-H., Dow, J. D., Benett, P. A. and Cahill, D. G. : Phys. Rev. B, **48**(1993), 2486
6) Tung, R. T. : Phys. Rev. Lett., **52**(1984), 461
7) van Loenen, E. J., Fischer, A. E. M. and van der Veen, J. F. : Surf. Sci., **155**(1985), 65
8) Iwami, M., Hashimoto, S. and Hiraki, A. : Solid State Commun., **49**(1984), 459
9) Giudice, M. D., Joyce, J. J., Ruckmann, M. W. and Weaver, J. H. : Phys. Rev. B, **35**(1987), 6213
10) Wallart, X., Nys, J. P., Zeng, H. S., Dalmai, G., Lefebvre, I. and Lannoo, M. : Phys. Rev. B, **41**(1990), 3087
11) van den Hoek, P. J., Ravenek, W. and Baerends, E. J., Phys. Rev. Lett., **25**(1988), 1743
12) Hocine, S. and Mathiot, D. : Appl. Phys. Lett., **53**(1988), 1269
13) Ishiyama, K., Taga, Y. and Ichimiya, A. : Phys. Rev. B, **51**(1995), 2380
14) Ed. Avouris, P. : "Atomic and Nanometer-Scale

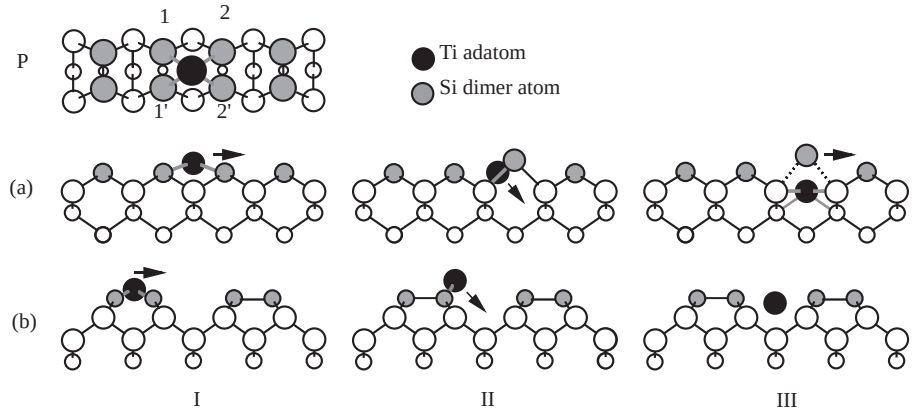

Fig. 5 Models for bonding sequence during site conversions (a) type-A and (b) type-B. P shows a plan view of the initial pedestal site adsorption. Displayed below are sectional views of sequences of atomic displacement projected to planes (a) parallel and (b) perpendicular to the dimer row.

Modification of Materials : Fundamentals and Applications", (1993), Kluwer Academic Publishers
15) Mo, Y. W., Kleiner, J., Webb, M. B. and Lagally, M. G. : Phys. Rev. Lett., **66**(1991), 1998
16) Ganz, E., Theiss, S. K., Hwang, I. S. and Golvochenko, J. : Phys. Rev. Lett., **68**(1992), 1567
17) Gomer, J. : Rep. Prog. Phys., **53**(1990), 917

Kengo Ishiyama was born in 1961. He received M. Eng. degree in applied physics in 1985 from Nagoya University. He belongs to the Thin Film Laboratory, where he works on micro-analytical studies of thin film growth. He is a member of The Physical Society of Japan and The Japanese Society of Applied Physics.

Yasunori Taga joined Toyota Central R & D Labs in 1970 after graduation from Nagoya Institute of Technology. He received Dr. Eng. in Materials Science from Osaka University in 1979. He became a manager of Electronics Device Division, where he works on thin film and surface and interface physics. He is a member of American Institute of Physics, American Vacuum Society, Materials Research Society, IEEE , and The Japanese Society of Applied Physics.

Ayahiko Ichimiya received M. Sci. degree in physics in 1966 from Gakushuin University and D. Sci. in physics in 1969 from Nagoya University. He joined Department of Applied Physics, School of Engineering, Nagoya University in 1969. He became a professor of Nagoya University in 1990.
He is a member of Material Research Society, The Japanese Society of Physics, The Japanese Society of Applied Physics, The Japanese Society of Surface Science, The Japanese Society of Crystallography, and The Japanese Society of Electron Microscopy.
He is also a consultant of commission of Electron Diffraction of The International Union of Crystallography.